HETEROCYCLES, Vol. 102, No. 10, 2021, pp. 1949 - 1968. © 2021 The Japan Institute of Heterocyclic Chemistry
Received, 8th June, 2021, Accepted, 9th July, 2021, Published online, 29th July, 2021.
DOI: 10.3987/COM-21-14503

# DESIGN AND ONE-POT SYNTHESIS OF SOME NEW [3,5-DI(4',5'-DIPHENYL-2'-SUBSTITUTED)-1*H*-IMIDAZOL-1-YL]]-1*H*-1,2,4-TRIAZOLE DERIVATIVES: *IN SILICO* ADMET AND DOCKING STUDY, ANTIBACTERIAL AND ANTIFUNGAL ACTIVITIES EVALUATION

**Nadia Hadhoum,[1]* Fatima Zohra Hadjadj-Aoul,[2] Smain Hocine,[3] Souhila Bouaziz-Terrachet,[4] Amar Abdoun,[5] Nacera Seklaoui,[6] Fella Boubrit,[5] Wissem Abderrahim,[6] and Lamine Redouane Mekacher[7]**

[1] Therapeutic Chemistry Laboratory, Department of Pharmacy, Faculty of Medicine, University Mouloud Mammeri 15000 Tizi-Ouzou Algeria. [2] Laboratory of Therapeutic Chemistry, Department of Pharmacy, Faculty of Medicine, University Ziania 16000 Algiers Algeria. [3] Laboratory of Applied Chemistry and Chemical Engineering Hasnaoua I, University Mouloud Mammeri 15000 Tizi-Ouzou Algeria. [4] Department of chemistry, faculty of Sciences, University of M'Hamed Bougara, Boumerdes (UMBB), Algeria. [5] Microbiology Service of CHU Tizi Ouzou, Algeria. [6] Parasitology-Mycology Service of CHU Tizi Ouzou, Algeria. [7] Medical Toxicology Service of CHU Tizi Ouzou, Algeria. *Corresponding author: E-mail address: nadia_hadhoum@yahoo.fr

**Abstract** – In this paper, a new series of some [3,5-di(4',5'-diphenyl-2'-substituted)-1*H*-imidazol-1-yl)]-1*H*-1,2,4-triazole derivatives (C1-C9) were efficiently synthesized by a one-pot three component reaction via a coupling of benzil, aldehydes and 3,5-diamino-1,2,4-triazole and using ceric ammonium nitrate as a catalyst. The structures of the newly compounds were investigated by IR, $^{1}$H NMR, $^{13}$C NMR and UV-visible spectroscopy. The *in vitro* antibacterial and antifungal activities showed that the C9 is the most active compound. The C9 docking study revealed the best mode of binding in the active site of the cytochrome P450 lanosterol 14α-demethylase. All the synthesized compounds were predicted as non-carcinogens and demonstrated acceptable pharmacokinetic profile in blood brain barrier (BBB) and human intestinal absorption (HIA).

## INTRODUCTION

Over the last few years, the frequency of fungal infections has increased significantly due to the progress of medical and surgical therapeutics, such as the use of vascular catheters, insertion of prostheses, and the prescription of large-spectrum antibiotics, causing an unstable flora leading to situations of immunological fragility, which may expose these patients to opportunistic agents. The fungal infections represent 5 to 10% of nosocomial infections widely recognized as one of the main causes of morbidity rate for immunodeficient patients.[1] In Algeria, around 1.41% of the total population has a serious fungal infection each year. Examples of deep mycosis are the candidemia and the invasive aspergillosis, the incidence of which is increasing among neutropenic patients in the north of the country reaching about 7.7% of the Algerian population of 42 million.[2]

The therapeutic arsenal currently available to combat these fungal infections consists of drug treatments often not devoid of secondary effects, represented by natural molecules such as griseofulvin, nystatin, amphotericin B, and molecules obtained by chemical synthesis, mainly azoles.[3] The discovery of the antifungal activity of azoles was a major advance in the treatment of superficial and systemic fungal infections. The first-generation azoles are imidazoles, of which clotrimazole and miconazole were the first representatives. Structural modifications on the latter have resulted in second-generation azoles, which are mainly topically active. Only miconazole and ketoconazole, which can be used for oral administration, have been able to treat deep fungal infections. Finally, third-generation azoles correspond to triazole derivatives such as fluconazole, itraconazole, voriconazole, posaconazole, etc,... Their pharmacological properties and their generally adequate tolerance make them appropriate for use in systemic fungal infections.[4,5]

Even though new antifungal drugs are appearing, the morbidity of fungal infections remains high, associated with the problem of emergence of resistance to antifungal agents, requiring the search for new classes of antifungal agents, with new therapeutic targets, or the synthesis of new molecules in currently known classes, mainly triazoles and imidazoles, which can be regarded as extremely important in many pharmaceutical applications. The nucleus 1,2,4-triazole exhibits a variety of pharmacological activities showing excellent antibacterial,[6-8] antifungal,[9-11] anti-tubercular,[12] anticancer,[13,14] anticonvulsant,[15] analgesic,[16] anti-inflammatory,[17] antidepressant,[18] antioxidant and antiviral activities.[19,20] The compounds containing an imidazole moiety possess the same biological properties such as antifungal,[21] antibacterial,[22] anticancer,[23] anti-inflammatory,[24] antiviral,[25] antitubercular,[26] anticonvulsant[27] and anticoagulants[28] activities. Different compounds containing an imidazole and a triazole have been synthesized and showed good biological properties in vitro, such as antifungal and antibacterial activities.[29,30] Although there is a diversity of antifungal molecules, the failure rate of antifungal treatments is still higher, and can be attributed to the involvement of new fungal species in immune-depressed patients, the increase in fungal

resistance, the bioavailability or toxicity of molecules, and the presence of many drug interactions,[31] implying the need for synthesizing new compounds in order to overcome these inconveniences.

The present paper studied the synthesis of new molecules combining both two imidazoles and one triazole. For this purpose, a new series of [3,5-di(4',5'-diphenyl-2'-substituted)-1*H*-imidazol-1-yl)]-1*H*-1,2,4-triazole derivatives were synthesized and the corresponding antibacterial and antifungal activities were evaluated**.**

A series of some [3,5-di(4',5'-diphenyl-2'-substituted)-1*H*-imidazol-1-yl)]-1*H*-1,2,4-triazole derivatives (C1-C9, Table 1) were obtained by condensation of benzil, corresponding aldehydes and 3,5-diamino-1,2,4-triazole, the rationality of the design and the synthesis of the newly compounds are shown in Scheme 1.

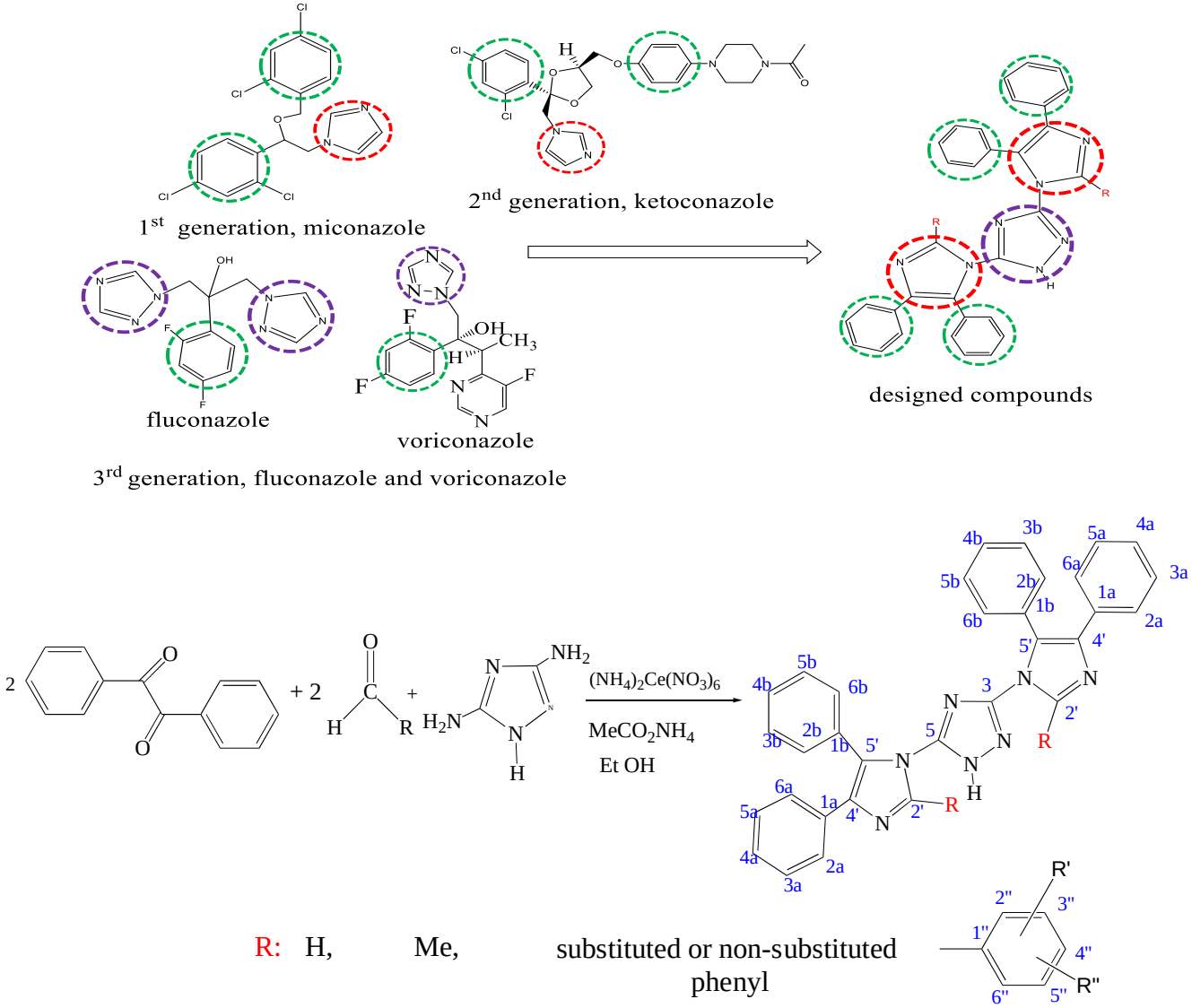


**Scheme 1.** Design and synthesis of [3,5-di (4',5'-diphenyl-2'-substituted)-1*H*-imidazol-1-yl)]-1*H*-1,2,4-triazole derivatives

## RESULTS AND DISCUSSION

### Chemistry

The compounds C1-C9 were synthesized in good yields ranging between 55% and 70%. The products were obtained according to the « Debus-Radziszewski » reaction. The newly synthesized compounds were insoluble in water, ethanol, ether and acetone; soluble in dimethylformamide (DMF) and dimethyl sulfoxide (DMSO). The physicochemical properties of C1-C9 are reported in Table 1. The UV-vis spectra after dissolution of the compounds (C1-C9) in DMSO showed one band for the products C1-C8 attributed to the π-π* transition (C = C or C = N) and three bands for C9, the first at 266 nm attributed to the π-π* transition (C = C or C = N), the second at 364 nm attributed to the n-π*, and the third at 424 nm attributed to the π-π* transition (N = O). The IR spectra revealed the main bands. The band at 3400 $cm^{-1}$ corresponding to the vibration (ν N-H), the band at 1600 $cm^{-1}$ related to (ν C=C), the elongation (ν C=N) was visualized at 1500 $cm^{-1}$ and the vibration corresponding to the aromatic protons (=C-H) between 3030 $cm^{-1}$ and 3080 $cm^{-1}$. The bands of the hydroxyls, the substituted amine and the nitro group, as well as the methyl, the unsubstituted phenyl and/or the polysubstituted phenyl were also identified. The structural features of these compounds were finely established based on $^{1}H$ NMR and $^{13}C$ NMR studies. The main features revealed in the $^{1}H$ NMR spectra are the singlet at $\delta_H$ 7.76 ppm corresponding to C-H of imidazole, visualized only on $^{1}H$ NMR of C1, it disappeared in the other molecules because of the substitution in 2' by an alkyl or phenyl; and a singlet at $\delta_H$ greater than 8 ppm, related to the N-H of triazole, obtained with all compounds. In all $^{1}H$ NMR spectra, we observed multiplets ranging between $\delta_H$ 7 ppm and $\delta_H$ 8 ppm suggesting the presence of aromatic protons of phenyls. The signal assigned to the protons of Me was detected in the up-field. Finally, the appearance of singlets at $\delta_H$ 9.79 ppm, $\delta_H$ 9.72 ppm and at $\delta_H$ 8.16 ppm suggests the presence of the hydroxyl on C4, C8 and C9 respectively. The proposed mechanism for the synthesis of (C1-C9) is shown in Scheme 2, it illustrates initially a protonation of the carbonyl of the aldehyde by ceric ammonium nitrate (CAN), which is followed by a nucleophilic attack by the doublet of the ammoniac nitrogen at the carbonyl of the aldehyde in order to form an imine intermediate; benzil and 3,5-diamino-1,2,4-triazole are involved in the second step.

### Protonation of the aldehyde by CAN and action of the ammoniac

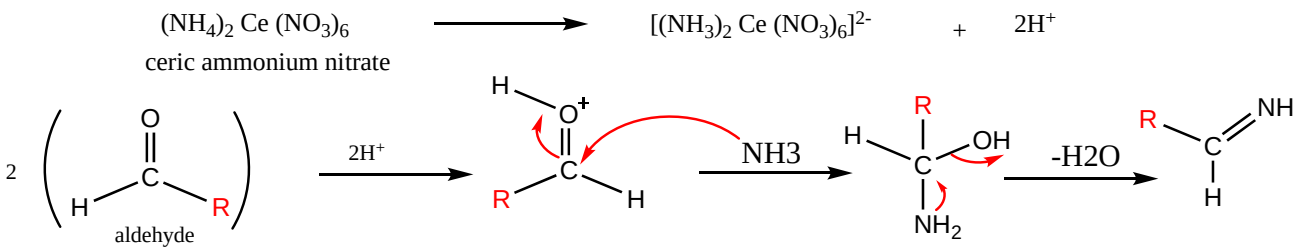

**Condensation with benzil and diaminotriazole**

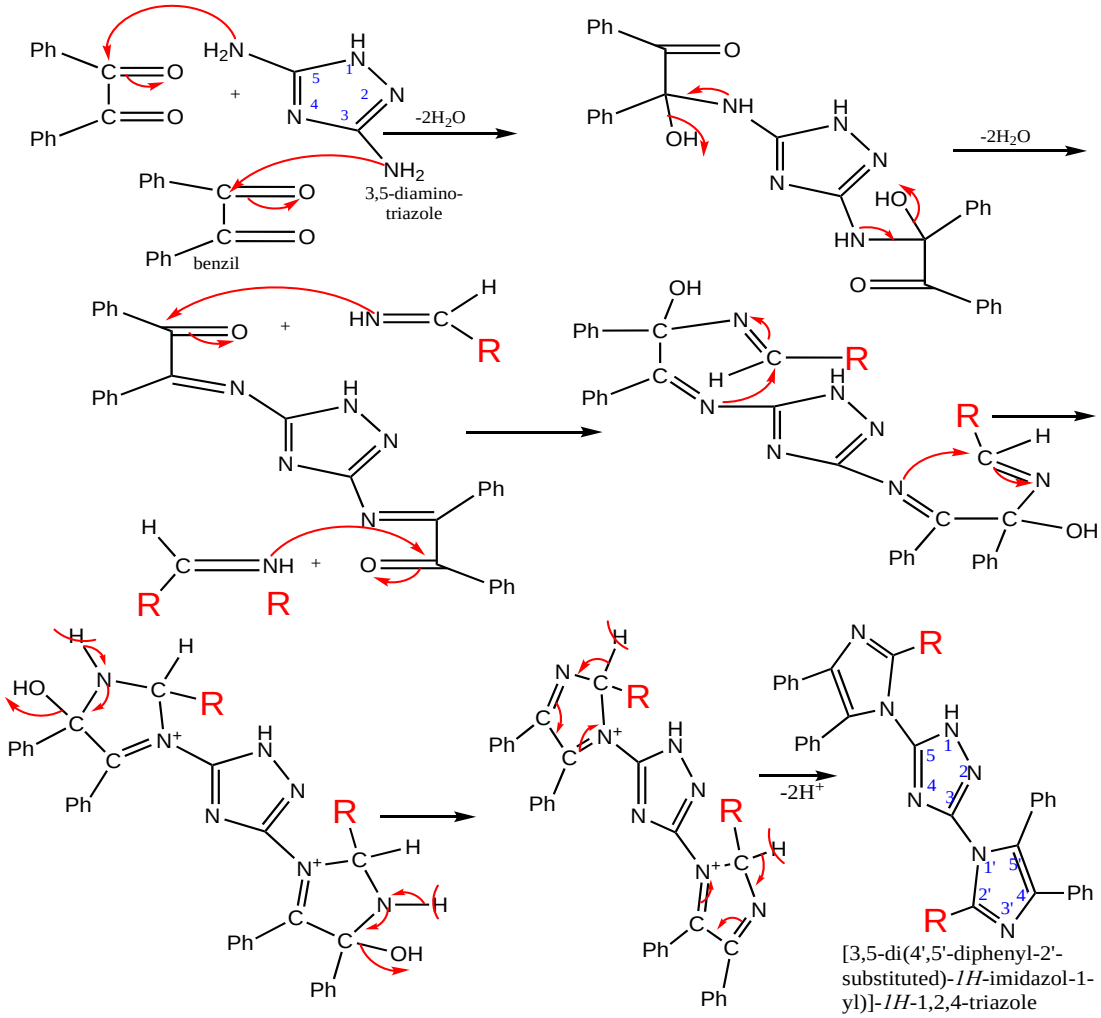


**Scheme 2.** Proposed mechanism for the synthesis of [3,5-di(4',5'-diphenyl-2'-substituted)-1*H*-imidazol-1-yl]]-1*H*-1,2,4-triazole derivatives

**Table 1.** Physicochemical data and UV-visible spectroscopic characteristics in DMSO of synthesized compounds (C1- C9)

| Compounds | Radical R | Yield (%) | physical appearance | λ abs max (nm) | | Mp (°C) | Rf* value |
|---|---|---|---|---|---|---|---|
| C1 | H | 70.13 | beige powder | 262 | π-π* (C = C or C = N) | 122-123 | 0.64 |
| C2 | Me | 62.90 | light yellow powder | 259 | π-π* (C = C or C = N) | 91-93 | 0.61 |
| C3 | Ph | 66.89 | fine beige crystals | 310 | π-π* (C = or C = N) | 280-283 | 0,61 |
| C4 |  | 56.96 | yellow powder | 258 | π-π* (C = C or C = N) | 206-209 | 0.61 |

| Compounds | Radical R | Yield (%) | physical appearance | λ abs max (nm) | | Mp (°C) | Rf* value |
|---|---|---|---|---|---|---|---|
| C5 | 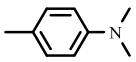 | 55.94 | yellow crystals | 368 | π-π* (C = C or C = N) | 269-271 | 0.62 |
| C6 | 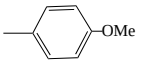 | 53.92 | yellow powder | 261 | π-π* (C = C or C = N) | 179-180 | 0,62 |
| C7 | 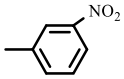 | 63.92 | yellow powder | 322 | π-π* (C = or C = N) | 286-289 | 0.62 |
| C8 | 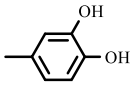 | 59.31 | dark green powder | 256 | π-π* (C = C or C = N) | 208-210 | 0.62 |
| C9 | 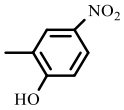 | 54.96 | orange powder | 266<br>364<br>424 | π-π* (C = C or C = N)<br>n-π*<br>π-π* (N = O) | 260-268 | 0.62 |

**: Rf in DMSO as solvent and (EtOH 75% - $Et_2O$ 25%) as eluent.*

**Biological activity and SAR analysis**

The *in vitro* study was carried out with three bacterial and seven fungal strains. The results (Table 2) showed an excellent antibacterial activity for C9 against *S. aureus* with an inhibition zone diameter of 32 mm and a MIC value of 32 µg/mL. The ATCC *S. aureus* being tested is a sensitive strain to Gentamycin with an inhibition zone diameter of 33 mm and a MIC value of 0.5 µg/mL.[32] On the other hand, the other compounds were inactive on this Gram positive bacteria. The newly synthesized compounds did not show any zone of inhibition against *E. coli* and *P. aerugenosa* and were completely inactive on the two Gram-negative bacteria tested. The results of *in vitro* antifungal activity are presented in Table 2 showing a good antifungal activity for C9 with a MIC below the value of 0.125 µg/mL for yeasts, *A. niger* and *M. gypseum*. The inhibition zones diameters were 24 mm for *C. albicans*, 19 mm for *C. neoformans*, 30 mm for *Trichopron* sp., 12 mm for *A. niger* and 16 mm for *M. gypseum*.

The *C. albicans* tested is a sensitive strain to fluconazole with an inhibition zone diameter of 32 mm and a MIC value of 4 µg/mL.[33] *Trichoporon* sp. was resistant to fluconazole showing a diameter of 30 mm with C9.[33] Fluconazole has no effect on *M. gypseum* while C9 showed an inhibition zone diameter of 16 mm. The compounds C2, C4, C5, C6 and C8 showed small inhibition zones diameters with a MIC below the value of 0.125 µg/mL for C2, C4, C6, C8 and 512 µg/mL for C5 respectively against *C. albicans*. The *C. neoformans* tested is a sensitive strain to fluconazole with an inhibition zone diameter of 34 mm and a MIC value of 8 µg/mL,[33] showing a small inhibition zones diameters and a MIC below the value of 0.125 µg/mL with C2, C4 and C8 and 512 µg/mL with C5 respectively. The *A. niger* tested is a resistant strain to fluconazole. The synthesized compounds did not show any inhibition zone against *A. flavus* and *M. canis*. The compounds C1, C3 and C7 were inactive against the fungal strains tested.

The relationship structure activity (SAR) analysis (Figure 1) revealed that the five compounds C2, C4, C6, C8, and C9, exhibited promising antifungal and antibacterial activities with the MIC values lower than 0.125 µg/mL. Further, the introduction of a methyl group at position 2' of two imidazole moieties, compound C2, showed the best antifungal and antibacterial activities than fluconazole. Also, the introduction of hydroxyphenyl, methoxyphenyl, and 3,4-dihydroxyphenyl groups at position 2' of the two imidazole moieties, accounts for promising antifungal and antibacterial activities (as in compounds C4, C6, C8, and C9, respectively). On the other hand, the introduction of 4-(dimethylamino)phenyl at position 2' of the two imidazole moieties, as in compound C5, did not show favorable effects on the antifungal and antibacterial activities (MIC = than 0.125 µg/mL). Interestingly, the compound C9 with 2-hydroxy-5-nitrophenyl group at position 2' of the two imidazole moieties showed promising antifungal and antibacterial activities against *Staphylococcus aureus*, *Candida albicans*, *Cryptococcus neoformans*, *Trichosporon* sp., *Aspergillus niger* and *Microsporum gypseum*.

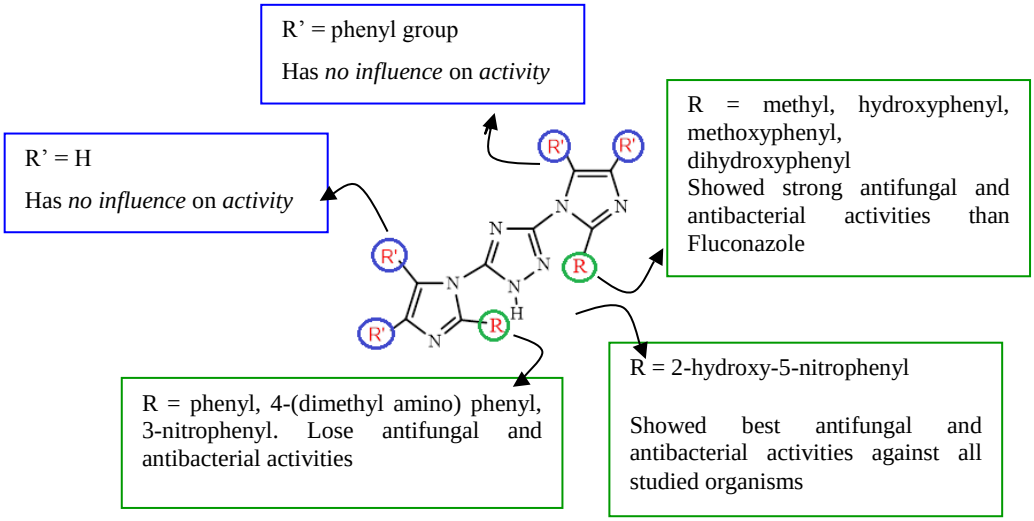


**Figure 1.** SAR of triazole derivatives as antifungal and antibacterial drugs

**Table 2.** *In vitro* antibacterial and antifungal activities of synthesized compounds and the controls

| Tested strains | Diameter of inhibition zones (mm) | | | | | |
|---|---|---|---|---|---|---|
| | ***C. albicans*** | ***C. neoformans*** | ***Trichoporon* sp.** | ***A. niger*** | ***M. gypseum*** | ***S. aureus*** |
| C1 | N. A. | N. A. | N. A. | N. A. | N. A. | N. A. |
| C2 | 9 (<0.125) | 7(< 0.125) | N. A. | N. A. | N. A. | N. A. |
| C3 | N. A. | N. A. | N. A. | N. A. | N. A. | N. A. |
| C4 | 9 (< 0.125) | 7(< 0.125) | N. A. | N. A. | N. A. | N. A. |
| C5 | 9 (512) | 9 (> 512) | N. A. | 8 (512) | N. A. | N. A. |
| C6 | 11 (< 0.125) | N. A. | N. A. | N. A. | N. A. | N. A. |
| C7 | N. A. | N. A. | N. A. | N. A. | N. A. | N. A. |
| C8 | 8 (< 0.125) | 9(< 0.125) | N. A. | N. A. | N. A. | N. A. |
| C9 | 24 | 19 (< 0.125) | 30 (< 0.125) | 12 | 16 | 32 (32) |

| Tested strains | Diameter of inhibition zones (mm) | | | | | |
|---|---|---|---|---|---|---|
| | ***C. albicans*** | ***C. neoformans*** | ***Trichoporon* sp.** | ***A. niger*** | ***M. gypseum*** | ***S. aureus*** |
| | (< 0.125) | | | (< 0.125) | (< 0.125) | |
| References* | 32 (4) | 34 (8) | N. A. | N. A. | N. A. | 33 (0.5) |
| DMSO | N. A. | N. A. | N. A. | N. A. | N. A. | N. A. |

** Antifungal: fluconazole; ATB: gentamycine, Values in brackets are MIC values (µg /mL)*
*N. A.: No Activity*

### *In silico* ADME and toxicity analysis

The *in silico* ADMET properties (absorption, distribution, metabolism, excretion, and toxicity) of of synthesized [3,5-di(4',5'-diphenyl-2'-substituted)-1*H*-imidazol-1-yl)]-1*H*-1,2,4-triazole derivatives were calculated using ADMET-Simulator[34] and reported in Table 3. All studied compounds were predicted as non-carcinogens, non-Renal Organic Cation Transporter (ROCTs), Weak Human Ether-a-go-go-Related Gene I (hERG) inhibitors and non hERG II inhibitors. All studied compounds were predicted as non-P-glycoprotein, non CYP3A4 inhibitors (except compounds C3, C5 and C6) and non-CYP450 2D6 inhibitors and substrates. In contrast, except compounds C7 and C9, all other compounds were predicted as inhibitors of CYP1A2 and CYP2C19. It may be recalled that the cytochrome P450 proteins play a vital role in metabolism and an inhibition of its isoforms would lead to drug interactions, accumulation and toxicity.[35] In addition, the inhibition of PG protein leads to interaction and accumulation of drug within the cells and produce cell toxicity.[36] On the other hand, compounds C5, C7, C8 and C9 demonstrated acceptable pharmacokinetic profile in blood brain barrier (BBB) and human intestinal absorption (HIA). Further, all studied compounds were predicted as low permeable in human adenocarcinoma cells (Caco-2). This property is the suitable tool used to analyze the metabolism and the transport of drugs.[37,38] The acceptable range of BBB for an ideal drug candidate is 0.73 to 0.91[39] and the acceptable range of Caco-2 permeability is between 0 poor absorption and +1 better absorption.[40] Finally, the model predicted the mitochondria as the most likely localization of studied compounds after their administration in the body.

**Table 3.** ADMET properties of studied compounds, predicted by admetSAR web server

| Compounds | C1 | C2 | C3 | C4 | C5 | C6 | C7 | C8 | C9 |
|---|---|---|---|---|---|---|---|---|---|
| Caco-2 permeability | 0.760 | 0.760 | 0.770 | 0.610 | 0.720 | 0.680 | 0.510 | 0.520 | 0.530 |
| HIA (% Absorbed) | 100 | 100 | 100 | 100 | 100 | 100 | 100 | 99.7 | 100 |
| P-glycoprotein I substrate | N. A. | N. A. | N. A. | N. A. | N. A. | N. A. | N. A. | N. A. | N. A. |
| P-glycoprotein I inhibitor | N. A. | N. A. | N. A. | N. A. | N. A. | N. A. | N. A. | N. A. | N. A. |

| Compounds | C1 | C2 | C3 | C4 | C5 | C6 | C7 | C8 | C9 |
|---|---|---|---|---|---|---|---|---|---|
| BBB permeability | 0.963 | 0.956 | 0.974 | 0.963 | 0.910 | 0.983 | 0.878 | 0.885 | 0.845 |
| Subcellular localization | Mit. | Mit. | Mit. | Mit. | Mit. | Mit. | Mit. | Mit. | Mit. |
| CYP1A2 inhibitior | Yes | Yes | Yes | Yes | Yes | Yes | N. A. | N. A. | N. A. |
| CYP2C19 inhibitior | Yes | Yes | Yes | Yes | Yes | Yes | N. A. | Yes | N. A. |
| CYP2D6 inhibitior | N. A. | N. A. | N. A. | N. A. | N. A. | N. A. | N. A. | N. A. | N. A. |
| CYP2D6 substrate | N. A. | N. A. | N. A. | N. A. | N. A. | N. A. | N. A. | N. A. | N. A. |
| CYP3A4 inhibitior | N. A. | N. A. | YES | N. A. | YES | YES | N. A. | N. A. | N. A. |
| hERG I inhibitor | Weak | Weak | Weak | Weak | Weak | Weak | Weak | Weak | Weak |
| hERG II inhibitor | N. A. | N. A. | N. A. | N. A. | N. A. | N. A. | N. A. | N. A. | N. A. |
| Carcinogens | N. A. | N. A. | N. A. | N. A. | N. A. | N. A. | N. A. | N. A. | N. A. |

Mit.: Mitochondria

**Molecular docking study**

To confirm the reliability of the docking model, the experimental ligand was docked in the active site of CYP51. The docked conformation was close to the experimental one, as shown in Figure 2a. Therefore, the developed model can be used to correctly predict the binding mode, energy and interaction with receptor.41

**Binding mode of studied compounds**

All the synthesized compounds were scored high values than standards drugs, fluconazole and voriconazole. C9 has shown the highest binding interaction energy -139.75 kcal/mol (Table 4). It is worth noting that, the negative values of docking energies change reveal that the binding process is spontaneous and the compound can be accepted as a drug.[42] Visualization of docked conformations of studied compounds shows that, unlike standard drugs voriconazole and fluconazole, most of the studied bind (C2 to C9) to the protein by blocking entry to the active site of CYP51 protein, as shown in Figure 2b.

The synthesized compounds are involved in hydrogen bond, non-covalent Pi-Pi T-shaped, Pi-Pi T-shaped, Pi-Alkyl and van der Waals interactions with amino acids residues of the CYP51 protein, as shown in Figure 2b, Figure 3 and table 4, while standards showed only hydrogen bond and van der Waals interactions. The residues His377, Ala61, Lys90, Leu88, Leu87, Ile231, Gln66, Ser506, Tyr505 are involved in hydrogen bonds with synthesized compounds. The phenyl ring at position 4’ of the first

imidazole (Figure 2b) ring is oriented toward the mouth of the CYP51 active site close to Tyr64, Phe380, Tyr65, Leu87 and His377 leading to favorable hydrophobic interactions and possibly to π-π interaction with Phe380.

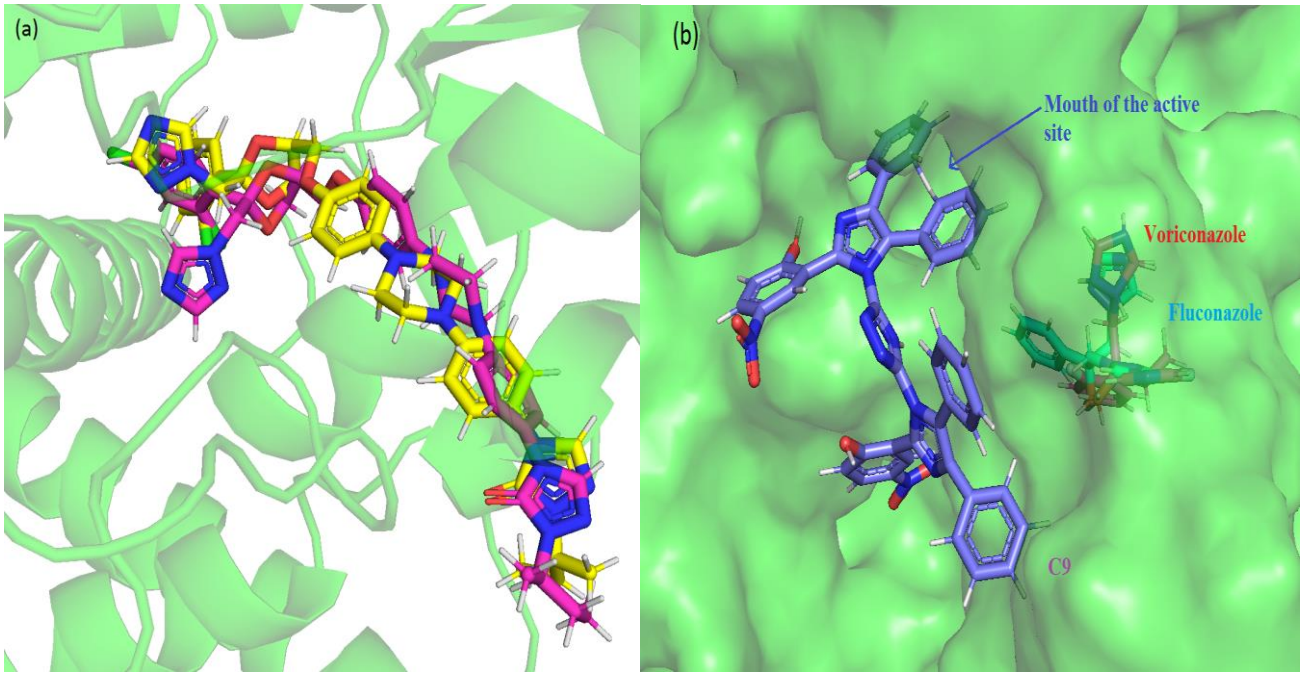


**Figure 2.** (a) Superposition of docked conformation and the X-ray structure of 1YN. (b) Binding mode of the compounds C9 (purple), fluconazole (red) and voriconazole (yellow). The protein backbone was presented in green ribbon (a) and green surface (b).

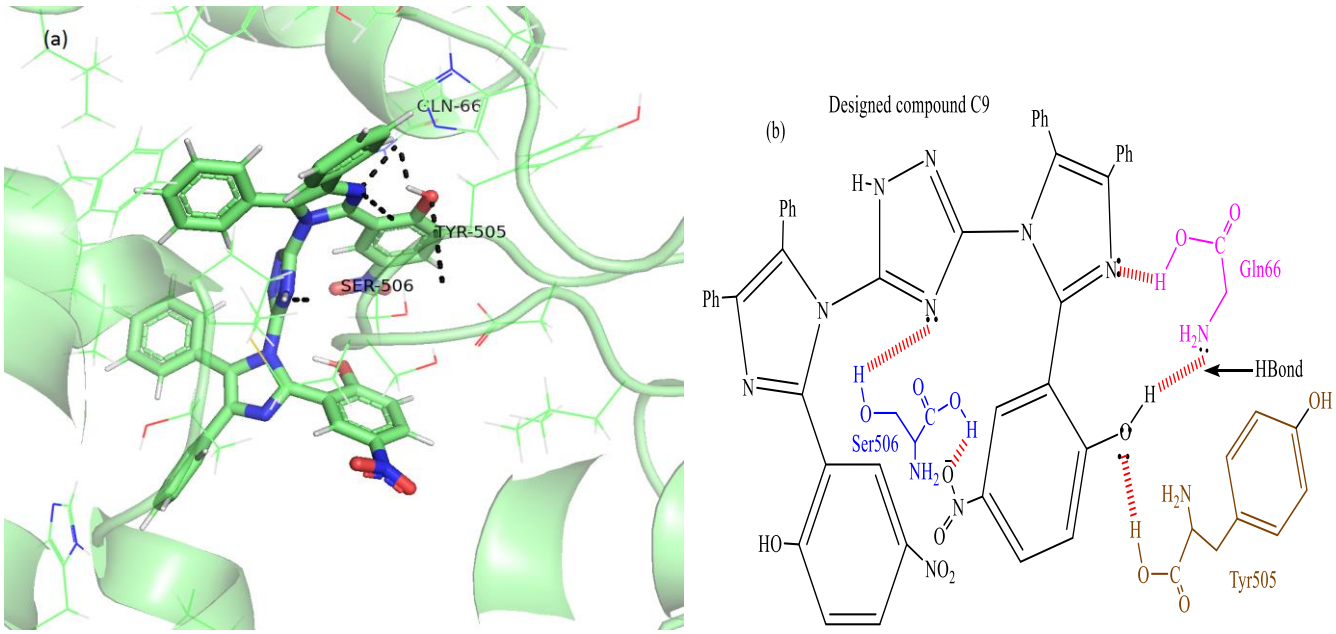


**Figure 3.** (a) and (b) Hydrogen bond interactions between CYP51 active site residues and designed compound C9. The protein backbone was presented in green ribbon (a).

**Table 4.** Hydrogen bonds interactions, interacting residues, and docking energies (kcal.mol$^{-1}$), calculated for synthesized compounds with the lanosterol 14α-demethylase cytochrome P450 (CYP51)

| Compounds | H-Bond | Interacting residues (< 4 Å) | Docking Energy |
|---|---|---|---|
| C2 | His377 (d = 3.1 Å, nitrogen imidazole ring)<br>Ala61 (d = 3.1 Å, carbonyl oxygen backbone) | Pi-Pi T-shaped: Tyr64<br>Pi-Alkyl: Leu87, Leu88, Phe58, Ala61, Ala62, Pro230,<br>van der Waals: Lys90, Phe233, Met92, Phe380, Ser378, Leu376, Val509, Met508, His377, Ser507, Tyr505, Gly65, Ser506, Gln66, | -133.95 |
| C4 | Lys90 (d = 2.7 Å, amino group of side chain)<br>Leu88 (d = 2.4 Å, carbonyl backbone)<br>Leu87 (d = 2.9 Å, carbonyl oxygen backbone) | Pi-Pi Stacked, Pi-Pi T-shaped: Phe233, Phe58, Phe235<br>Pi-Alkyl: Ala61, Pro230, Leu87, Val234<br>van der Waals: Met508, Ser378, Phe380, His377, Ser507, Tyr64, Ile231, Trp57, Gln66, Ala62 | -131.82 |
| C5 | Ser506 (d = 3.1 Å, carbonyl oxygen backbone) | Pi-Pi T-shaped: Phe58, His377, Phe380<br>Pi-Alkyl: Leu88, Val510, Phe233<br>Pi-lone Pair: Ser507<br>van der Waals: Gln66, Phe235, Ala62, Trp57, Ala61, Pro375, Ile231, Val509, Met508, Ser378, Ile379, Tyr118, Met92, Lys90 | -128.91 |
| C6 | His377 (d = 2.9 Å, nitrogen imidazole ring)<br>Ile231 (d = 2.7 Å, carbonyl oxygen backbone) | Pi-Pi Stacked, Pi-Pi T-shaped: Phe233, Phe380, Phe235<br>Pi-Alkyl: Ala61, Pro230, Ala117, Val234<br>van der Waals: Phe235, Ile231, Ala61, Ala62, Gln66, Ser507, Ser506, Gly65, Tyr64, His377, Tyr505, Ser378, Met508, Tyr64, | -135.38 |
| C8 | Gln66 (d = 2.7 Å, amino group of side chain)<br>Ser506 (d = 2.6 Å, hydroxyl group of side chain)<br>Tyr505 (d = 2.6 Å, carbonyl oxygen backbone)<br>Leu87 (d = 2.4 Å, carbonyl oxygen backbone) | Amide-Pi stacked and Pi-Pi T-shaped: Ser507, His377, Phe380, Phe58<br>Pi-alkyl: Leu88, Ile231, Pro230, Leu376<br>van der Waals: Trp57, Phe235, Val234, Asn232, Val510, Val509, Met508, Ile379, Tyr118, Ser378, Tyr64, Asp504, Met92 | -139.67 |
| C9 | Gln66 (d = 2.3 Å, carbonyl oxygen backbone, d = 2.4 Å amino group of side chain)<br>Tyr505 (d = 1.9 Å, carbonyl oxygen | Pi-sigma: Gly65, Pro230,<br>Pi-lone pair: His377<br>Pi-Pi T-shaped and Pi-Pi Stacked: Tyr64, Phe233<br>Pi-Alkyl: Pro68, Ala61<br>van der Waals:Phe58, Ala62, Trp57, | -139.75 |

| Compounds | H-Bond | Interacting residues (< 4 Å) | Docking Energy |
|---|---|---|---|
| | backbone)<br>Ser506 (d = 2.6 Å, hydroxyl group of side chain, d = 2.1 Å, carbonyl oxygen atom of backbone) | Thr229, Phe235, Val234, Leu88, Leu87, Lys90, Met508, Ser378, Ser507, Met92, Val510, Ser506 | |
| Fluconazole | Tyr118 (d = 3.1 Å, hydroxyl group of side chain)<br>Gly308 (d = 3.0 Å, carbonyl oxygen backbone) | van der Waals: Ile471, Ile131, Phe380, Thr311, Val509, His310, Met508, Phe228, Gly307, Gly308, Gly303 | -124,14 |
| Voriconazole | Gly303(d = 2.2 Å, carbonyl oxygen backbone)<br>Ile304 (d = 2.0 Å, carbonyl oxygen backbone) | van der Waals: Phe475, Leu150, Gly307, Met306, Ala146, Phe126, Leu305, Gln309, Leu300, Tyr132, Lys143, Cys470, Thr311, Gly308, | -107,08 |

## CONCLUSION

In the present study, a series of some new [3,5-di(4',5'-diphenyl-2'-substituted)-1*H*-imidazol-1-yl)]-1*H*-1,2,4-triazole derivatives were synthesized by a one-pot multi-component reaction, easy to achieve experimentally and meeting environmental and economic requirements such as reduction of synthesis steps and the use of efficient catalysts. The structures of synthesized compounds were performed by UV-visible, IR, $^{1}$H NMR and $^{13}$C NMR. The *in vitro* antibacterial activity, *in silico* ADMET and docking study were performed and discussed. The compound C9 was the most active; it showed good antibacterial and antifungal activities against some strains with an acceptable pharmacokinetic profile. The docking study predicted that it can bind freely to the target of azoles by generating hydrogen bonds, non-covalent Pi-Pi T-shaped, Pi-Pi T-shaped, Pi-Alkyl and van der Waals interactions with the target. The *in vitro* results are in concordance with the molecular docking studies. As part of our study, some nitrogen heterocycles were associated in the form of two imidazoles (ancient antifungals) and a triazole (new products) aiming to obtain new substances with an optimal biological activity and which can constitute potential drug candidates.

## EXPERIMENTAL

### General procedure for the synthesis of [3,5-di(4',5'-diphenyl-2'-substituted)-1*H*-imidazol-1-yl)]-1*H*-1,2,4-triazole derivatives (C1-C9)

A mixture of corresponding aldehydes (0.02 mol), benzil (0.02 mol) and 3,5-diamino-1,2,4-triazole (0.01 mol), in EtOH at reflux conditions was stirred in the presence of CAN (30%: mole percent) as a catalyst at 95-100 °C for 3 h.[30] The residue was later cooled to ambient temperature. The resulting solid separated was collected by filtration and recrystallized from EtOH to afford the desired compound. The reaction was monitored by TLC (EtOH 75% - $Et_2O$ 25%).

### C1: 3,5-Di(4',5'-diphenyl-1*H*-imidazol-1-yl)-1*H*-1,2,4-triazole

Yield 70%; mp 122-123 °C; UV-visible (DMSO) λmax 262nm (C=C, C=N); IR (KBr, υ, $cm^{-1}$): 3405 (NH), 1301 (C-N), 1440 and 1590 (2C=N), 1163 (N-N), 1671 (C=$C_{aryl}$), 3081 (=CH); $^1$H NMR (400 MHz DMSO-$d_6$) δ ppm: 7.62-7.65 (8H, m, Ar-H), 7.76 (2H, s, C-H imidazole), 7.78-7.82 (4H, m, Ar-H), 7.91-7.94 (8H, m, Ar-H), 7.99 (s, 1H, N-H triazole); $^{13}$C NMR (DMSO-$d_6$) δ ppm: 129.9 ($C_{2a}$-$C_{6a}$, $C_{2b}$-$C_{6b}$), 130 ($C_{1a}$, $C_{1b}$), 132.6 ($C_{2'}$), 135.9 ($C_{4'}$, $C_{5'}$), 195.1 ($C_3$, $C_5$).

### C2: 3,5-Di(2'-methyl-4',5'-diphenyl-1*H*-imidazol-1-yl)-1*H*-1,2,4-triazole

Yield 62%; mp 91-93 °C; UV-visible (DMSO) λmax 259nm (C=C, C=N); IR (KBr, υ, cm-$^1$): 3434 (NH), 1219 (C-N), 1594 (C=N), 1076 (N-N), 1671 (C=$C_{aryl}$), 3065 (=CH), 2927 (-CH); $^1$H NMR (400 MHz DMSO-$d_6$) δ ppm: 2.49 (6H, s, CH3), 7.79-7.92(20H, m, Ar-H), 7.94(1H, s, N-H triazole); $^{13}$C NMR (DMSO-$d_6$) δ ppm: 39 ($CH_3$), 129.9 ($C_{2a}$-C6a, C2b-C6b), 130 ($C_{1a}$, $C_{1b}$), 132.8 ($C_{2'}$), 135.99 ($C_{4'}$, $C_{5'}$), 195.1 ($C_3$, $C_5$).

### C3: 3,5-Di(2',4',5'-triphenyl-1*H*-imidazol-1-yl)-1*H*-1,2,4-triazole

Yield 66%; mp 280-283 °C; UV-visible (DMSO) λmax 310nm (C=C, C=N); IR (KBr, υ, $cm^{-1}$): 3451 (NH), 1313 (C-N), 1440 and 1590 (2C=N), 1153 (N–N), 1671 (C=$C_{aryl}$), 3063 (=CH); $^1$H NMR (400 MHz DMSO-$d_6$) δ ppm: 7.62-7.66 (12H, m, Ar-H), 7.78-7.83 (6H, m, Ar-H), 7.92-7.95(12H, m, Ar-H), 9.27 (1H, s, N-H triazole); $^{13}$C NMR (DMSO-$d_6$) δ ppm: 129.9 ($C_{2a}$-$C_{6a}$, $C_{2b}$-$C_{6b}$, $C_{2''}$-$C_{6''}$), 130 ($C_{1a}$, $C_{1b}$, $C_{1''}$), 132.6 ($C_{2'}$), 136 ($C_{4'}$, $C_{5'}$), 195.7 ($C_3$, $C_5$).

### C4: 3,5-Di[2'((4"-hydroxy)phenyl)-4',5'-diphenyl-1*H*-imidazol-1-yl]-1*H*-1,2,4-triazole

Yield 56%; mp 206-209 °C; UV-visible (DMSO) λmax 258nm (C=C, C=N); IR (KBr, υ, $cm^{-1}$) : 3441

(NH), 1452 and 1584 (2C=N), 1025 (N–N), 1665 (C=$C_{aryl}$), 3167 and 1381 (-OH), 1218 (C-O), 3056 (=CH); $^{1}$H NMR (400 MHz DMSO-$d_6$) δ ppm: 7.62-7.66 (20H, m, Ar-H), 7.78-7.83 (4H, m, Ar-H), 7.92-7.94 (4H, m, Ar-H), 9.79 (2H, s, O-H), 10.57 (1H, s, N-H triazole); $^{13}$C NMR (DMSO-$d_6$) δ ppm: 115.3 ($C_{4a}$, $C_{4b}$), 116.1($C_{5a}$, $C_{6a}$, $C_{5b}$,$C_{6b}$), 127.1 ($C_{3a}$, $C_{3b}$), 128.6 ($C_{2a}$, $C_{2b}$), 129.1 ($C_{2''}$, $C_{6''}$), 129.6 ($C_{4'}$, $C_{5'}$), 130.4 ($C_{1a}$, $C_{1b}$), 132.7 ($C_{2'}$), 136 ($C_3$, $C_5$), 163.6 ($C_{1''}$), 191.3 ($C_{3''}$, $C_{5''}$), 196.3 ($C_{4''}$).

**C5: 3,5-Di[2'((4”-(*N*,*N*-dimethyl)amino)phenyl)-4',5'-diphenyl-1*H*-imidazol-1-yl]-1*H*-1,2,4- triazole**

Yield 55%; mp 269-271 °C; UV-visible (DMSO) λmax 368nm (C=C; C=N); IR (KBr, υ, cm$^{-1}$) : 3459(NH), 1327 (C-N), 1594 (C=N), 1011 (N-N), 1670 (C=$C_{aryl}$), 3066 (=CH), 2914 (aliphatic C-H), 1220 and 1178 (C-N), 1404 and 1454 (CH3); $^{1}$H NMR (400 MHz DMSO-$d_6$) δ ppm: 3.01(12H, s, CH3), 7.60-7.82 (20H, m, Ar-H), 7.92-7.95(8H, m, Ar-H), 8.84(1H, s, NH triazole); $^{13}$C NMR (DMSO-$d_6$) δ ppm: 25.72 ($CH_3$), 111.8 ($C_{3''}$, $C_{5''}$), 123.3 ($C_{2''}$, $C_{6''}$), 129.7 ($C_{2a}$-$C_{6a}$, $C_{2b}$-$C_{6b}$), 130.7 ($C_{1''}$), 132.4 ($C_{1a}$, $C_{1b}$), 135.9 ($C_{4'}$, $C_{5'}$), 153.1 ($C_{2'}$), 161.8 ($C_3$, $C_5$), 195 ($C_{4''}$).

**C6: 3,5-Di[2'((4''-methoxy)phenyl)-4',5'-diphenyl-1*H*-Imidazol-1-yl]-1*H*-1,2,4-triazole**

Yield 53%; mp 179-180 °C; UV-visible (DMSO) λmax 261nm (C=C, C=N); IR (KBr, υ, cm$^{-1}$) : 3422 (NH), 1381 (C-N), 1453 and 1582 (2C=N), 1015 (N-N), 1670 (C=$C_{aryl}$), 3047 (=CH), 2965 (aliphatic C-H), 1229 (C-O) ; $^{1}$H NMR (400 MHz DMSO-$d_6$) δ ppm: 3.82 (6H, s, O-CH3), 7.62-7.82 (20H, m, Ar-H), 7.92-7.94 (8H, m, Ar-H), 8.95 (1H, s, NH triazole); $^{13}$C NMR (DMSO-$d_6$) δ ppm: 55.5 (O-CH3), 114.5 ($C_{3''}$, $C_{5''}$), 127.1 ($C_{1a}$, $C_{1b}$), 128.6 ($C_{2a}$-$C_{6a}$, $C_{2b}$-$C_{6b}$), 131 ($C_{1''}$), 132.4 ($C_{2''}$, $C_{6''}$), 136.3 ($C_{4'}$, $C_{5'}$), 146.1 ($C_{2'}$), 160.1 ($C_3$, $C_5$), 196.14 ($C_{4''}$).

**C7: 3,5-Di[2'((3''-nitro)phenyl)-4',5'-diphenyl-1*H*-imidazol-1-yl]-1*H*-1,2,4 triazole**

Yield 63%; mp 286-289 °C; UV-visible (DMSO) λmax 322nm (C=C, C=N); IR (KBr, υ, cm$^{-1}$) : 3446 (NH), 1341 (C-N), 1519 and 1594 (2C=N), 1057 (N-N), 1670 (C=$C_{aryl}$), 3097 (=CH), 1391 (NO2); $^{1}$H NMR (400 MHz DMSO-$d_6$) δ ppm: 7.56-7.94 (20H, m, Ar-H), 8.18-8.74(8H, m, Ar-H), 8.95(1H, s, NH triazole); $^{13}$C NMR (DMSO-$d_6$) δ ppm: 119.2 ($C_{2''}$), 122.7 ($C_{4''}$), 125.8 ($C_{2a}$, $C_{6a}$, $C_{2b}$, $C_{6b}$), 128.9 ($C_{4a}$, $C_{4b}$), 129.7 ($C_{3a}$, $C_{5a}$, $C_{3b}$, $C_{5b}$), 131 ($C_{1''}$), 135.6 ($C_{5''}$, $C_{6''}$), 138 ($C_{1a}$, $C_{1b}$), 143.7 ($C_{2'}$), 148.6 ($C_{3''}$), 159.4 ($C_3$, $C_5$).

**C8: 3,5-Di[2'((3'',4''-dihydroxy)phenyl)-4',5'-diphenyl-1*H*-imidazol-1-yl]-1*H*-1,2,4-triazole**

Yield 59%; mp 208-210 °C; UV-visible (DMSO) λmax 256nm (C=C, C=N); IR (KBr, υ, cm$^{-1}$) : 3447 (NH), 1391 (C-N), 1585 (C=N), 1005 (N-N), 1645 (C=$C_{aryl}$), 3016 (=CH), 3148 (-OH), 1229 (C-O); $^{1}$H

NMR (400 MHz DMSO-$d_6$) δ ppm: 7.62-7.66 (20H, t, *J*=7.64, Ar-H), 7.79-7.82 (4H, t, *J*=7.80, Ar-H), 7.92- 7.94 (2H, d, *J*=7.93, Ar-H), 9.72 (4H, s, O-H), 12.12 (1H, s, N-H triazole); $^{13}$C NMR (DMSO-$d_6$) δ ppm: 127 ($C_{2''}$, $C_{5''}$), 127.7 ($C_{6''}$), 128.5 ($C_{1''}$), 128.7 ($C_{2a}$- $C_{6a}$, $C_{2b}$- $C_{6b}$), 129.8 ($C_{1a}$, $C_{1b}$), 130.7 ($C_{4'}$, $C_{5'}$), 132.6 ($C_{2'}$), 135.8 ($C_{3''}$, $C_{4''}$), 196.2 ($C_3$, $C_5$).

**C9: 3,5-Di[2'((2''-hydroxy-5''-nitro)phenyl)-4',5'-diphenyl-1*H*-imidazol-1-yl]-1*H*-1,2,4-triazole**

Yield 54%; mp 260-268 °C; UV-visible (DMSO) λmax 266, 364 and 424 nm (C=C, C=N, N=O); IR (KBr, υ, $cm^{-1}$): 3448 (NH), 1391 (C-N ; NO2), 1644 (C=N; $C=C_{aryl}$), 3080 (=CH), 3200 (-OH), 1097 (C-O); $^1$H NMR (400 MHz DMSO-$d_6$) δ ppm: 7.35-7.66 (m, 20H, Ar-H), 7.79-7.82 (2H, m, Ar-H), 7.92-7.94 (4H, m, Ar-H), 8.16 (2H, s, O-H), 8.19 (1H, s, N-H triazole); $^{13}$C NMR (DMSO-$d_6$) δ ppm: 128.2 ($C_{3''}$), 128.4 ($C_{1''}$), 128.9 ($C_{6''}$), 129.1 ($C_{4''}$), 129.9 ($C_{2a}$-$C_{6a}$, $C_{2b}$-$C_{6b}$), 130 ($C_{1a}$, $C_{1b}$), 132.8 ($C_{4'}$, $C_{5'}$), 136.3 ($C_{5''}$), 160.4 ($C_{2'}$), 172.7 ($C_3$, $C_5$), 196.4 ($C_{2''}$).

**Biological activity**

**Disc diffusion antibiogram and antifungal susceptibility testing**

The different compounds C1-C9 were screened *in vitro* against two Gram-negative bacteria *Escherichia coli* (ATCC 25922) and *Pseudomonas aeruginosa* (ATCC 27853), and also against a Gram-positive bacteria *Staphylococcus aureus* (ATCC 25923) by the disc diffusion method as described in the National Committee for Clinical and Laboratory Standards.[32] From a pure culture of 18 to 24 h, some isolated and perfectly identical colonies were scraped with a platinum loop and introduced in a 5 to 10 mL of 0.9% sterile physiological water. The turbidity of this microbial suspension was homogenized and adjusted to 0.5 MF (McFarland), dilute to 1/10th. The bacterial solution was inoculated in the Müller-Hinton agar medium by swabbing with Petri dishes at room temperature. The tested compounds were dissolved in DMSO with a 5.12 mg/mL concentration. 10 µL of tested sample were poured onto paper disks 6 mm in diameter, which have been delicately placed on the surface of the agar plates. These were later maintained at 37 °C for 24 h. Activities determination was carried out by measuring the diameter of the inhibition zone (mm). Controls cultures without antibiotics and with Gentamycin were also performed. The gentamicin was dissolved in sterile physiological water.

The synthesized compounds were evaluated for their antifungal activity against *Candida albicans* (laboratory isolate), *Cryptococcus neoformans* (laboratory isolate), *Trichosporon* sp. (laboratory isolate), *Aspergillus niger* (ATCC 16404), *Aspergillus flavus* (laboratory isolate), *Microsporum gypseum* (laboratory isolate) and *Microsporum canis* (laboratory isolate). The casitone agar was used and the disk

diffusion method was carried out in conformity with the agar gel diffusion test used in clinical microbiology.[32] The synthesized compounds were dissolved in DMSO. The fungal strains tested were 48 h cultures for *Candida albicans* and *Trichosporon* sp., 72 h cultures for *Cryptococcus neoformans*, 48 h to 5 days cultures for *Aspergillus* and 15 days cultures for *Dermatophytes*. The colonies were suspended in 5 to 10 mL of 0.9% sterile physiological water, and the turbidity was adjusted to yield of 0.5 $10^3$ UFC/mL (0.5 McFarland standard) for *yeasts* and 0.4 $10^4$ UFC/mL for *Aspergillus* and *Dermatophytes*.[33,43,44] The *Candida albicans* and *Trichosporon* sp. were incubated at 35 °C for 24 to 48 h, the *Cryptococcus neoformans* at 35 °C for 72 h, the *Aspergillus* at 35 °C for 48 h to 5 days and finally the *Dermatophytes* at 28 °C for 15 days. The media with DMSO and the media with fluconazole were set up as controls.

**Determination of minimum inhibitory concentration (MIC)**

The half-logarithmic dilutions (from half to half) were carried out, in the DMSO of the solution at 5120 μg/mL, up to the final concentration of 1.25 μg/mL. 2 mL of each dilution with 18 mL of liquefied Müller-Hinton medium were first homogenized on a petri dish, to obtain a final concentration ranging from 512 μg/mL to 0.125 μg/mL. The petri dishes were carried out with dilutions of gentamicin and petri dish without any dilutions as control. 2 μL of each bacterial inoculum at 0.05 MF were placed and the petri dishes were incubated at 37 °C for 24 h. The MIC, which represents the lowest concentration that inhibits visible bacterial growth, was noted. For the fungal strains, as was the case of MICs for bacteria, the *yeasts*, and *Aspergillus* were incubated at 35 °C and the *Dermatophytes* at 28 °C. The growth MIC was determined for *C. albicans* and *Trichosporon* sp. at 24 to 48 h, *C. neoformans* at 72 h, *Aspergillus* at 5 to 7 days, and *Dermatophytes* at 15 days. The casitone agar was used and the fluconazole was carried out as a control.

***In silico* ADMET study**

In modern drug discovery, the behavior in the body of new drug candidate can be predicted using modeling and computer simulations before experimental testing in vivo. For this purpose, ADMET-Simulator was performed to predict ADMET properties (absorption, distribution, metabolism, excretion and toxicity).[34] ADMET-Simulator is a chemoinformatics-based toolbox that can predict about 50 ADMET endpoints using high quality and predictive QSAR models. Several pharmacodynamic and pharmacokinetic properties were calculated such as carcinogenicity,[45] acute oral toxicity, Renal Organic Cation Transporter, CaCo-2 permeability,[46] Blood-brain barrier (BBB) permeability,[47] human intestinal absorption (HIA),[48] P-glycoprotein inhibitor and substrate,[49] inhibition of cytochrome P450 isoform

CYP1A2, CYP2C19, CYP2D6[50] and inhibition Human of Ether-a-go-go-Related Gene I and II (hERG) of the studied compounds.

**Molecular docking study**

Azoles antifungal act by competitive inhibition of the lanosterol 14α-demethylase cytochrome P450 (CYP51).[51] So, we used Docking software iGEMDOCK[52] to predict the binding mode, docking energies and binding interactions between the active site residues of the CYP51 protein and the synthesized compounds. The protein coordinates was downloaded from Protein Data Bank (http://www.rcsb.org/) (PDB : 5V5Z with resolution of 2.90 Å, corresponding to CYP51 complexed with azole drug 1YN.[53] Two antifungal drugs namely voriconazole and fluconazole were used as references and were similarly docked into the active site of the receptor. Synthesized compounds and standard drugs were drawn using MarvinSketch software.[54] The PDB file of each compound was imported in iGEMDOCK software as ligand. As done in previous studies,[55] the active site was identified as a distance 8Å from the center of bound ligand 1YN. All docking simulations were performed with accurate docking, population size of 800, 80 generations and number of solutions of 10. iGEMDOCK ranks and visualizes the screening compounds by combining the pharmacological interactions and energy-based scoring function. Obtained binding mode and docking energies of each compound was compared with those of the standards drugs.

**ACKNOWLEDGEMENTS**

The authors acknowledge the head of the service of the microbiology and mycology laboratories of the CHU Nedir Mohamed of Tizi Ouzou in Algeria and the staff of laboratory of Applied Chemistry and Chemical Engineering (LCAGC) of the University Mouloud Mammeri of Tizi-Ouzou Algeria for their contributions.

**REFERENCES AND NOTES**

1. A. Schrapp and F. Lamoureux, Chapter 14 in *Pharmacologie des Anti-Infectieux*, 2018, pp. 115-120.
2. M. Chekiri-Talbi and D. W. Denning, *J. Myco. Med.*, 2017, **27**, 139.
3. A. Denieul and S. Faure, *Actual. Pharm.*, 2009, **48**, 14.
4. É. Penet, L. Bonneau, A.-S. Parinaud, S. Gonnin, M.-A. Gaillard, and M. Javerliat, *Actualit. Pharm. Hosp.*, 2011, **7**, 10.
5. M. Mallié and J.-M. Bastide, *Rev. Francoph. des Lab.*, 2001, **2001**, 63.
6. S.-F. Barbuceanu, G. L. Almajan, I. Saramet, C. Draghici, A. I. Tarcomnicu, and G. Bancescu, *Eur. J. Med. Chem.*, 2009, **44**, 4752.
7. F. Gao, T. Wang, J. Xiao, and G. Huang, *Eur. J. Med. Chem.*, 2019, **173**, 274.

8. J. Zhang, S. Wang, Y. Ba, and Z. Xu, *Eur. J. Med. Chem.*, 2019, **174**, 1.
9. J. Wu, T. Ni, X. Chai, T. Wang, H. Wang, J. Chen, Y. Jin, D. Zhang, S. Yu, and Y. Jiang, *Eur. J. Med. Chem.*, 2018, **143**, 1840.
10. Z. Ding, T. Ni, F. Xie, Y. Hao, S. Yu, X. Chai, Y. Jin, T. Wang, Y. Jiang, and D. Zhang, *Bioorg. Med. Chem. Lett.*, 2020, **30**, 126951.
11. S. Wu, W. Zhang, L. Qi, Y. Ren, and H. Ma, *J. Mol. Struct.*, 2019, **1197**, 171.
12. M. V. Papadopoulou, W. D. Bloomer, and H. S. Rosenzweig, *Bioorg. Med. Chem.*, 2017, **25**, 6039.
13. M. Reda Aouad, H. Musallam Al-Mohammadi, F. Faleh Al-blewi, S. Ihmaid , H. Mostafa Elbadawy, S. Saad Althagfan, and N. Rezki, *Bioorg. Chem.*, 2020, **94**, 103446.
14. M. M. Slaihim, F. S. R. Al-Suede, M. Khairuddean, M. B. K. Ahamed, and A. M. S. A. Majid, *J. Mol. Struct.*, 2019, **1196**, 78.
15. B. Kaproń, J. J. Łuszczki, A. Siwek, T. Karcz, G. Nowak, M. Zagaja, M. Andres-mach, A. Stasiłowicz, J. Cielecka-Piontek, J. Kocki, and T. Plech, *Bioorg. Chem.*, 2020, **94**, 103355.
16. A. M. Vijesh, A. M. Isloor, P. Shetty, S. Sundershan, and H. K. Fun, *Eur. J. Med. Chem.*, 2013, **62**, 410.
17. A. N. Boshra, H. H. Abdu-Allah, A. F. Mohammed, and A. M. Hayallah, *Bioorg. Chem.*, 2020, **95**, 103505.
18. X.-Q. Deng, M.-X. Song, Y. Zheng, and Z.-S. Quan, *Eur. J. Med. Chem.*, 2014, **73**, 217.
19. B. M. Geetha, K. N. Brinda, G. Achar, J. G. Małecki, M. Alwarsamy, V. S. Betageri, and S. Budagumpi, *J. Mol. Liq.*, 2020, **301**, 112352.
20. X. Cao, W. Wang, S. Wang, and L. Bao, *Eur. J. Med. Chem.*, 2017, **139**, 718.
21. M. Bolous, N. Arumugam, A. I. Almansour, R. S. Kumar, K. Maruoka, V. C. Antharam, and S. Thangamani, *Bioorg. Med. Chem. Lett.*, 2019, **29**, 2059.
22. S. Sharma, S. Gangal, and A. Rauf, *Eur. J. Med. Chem.*, 2009, **44**, 1751.
23. A. Negi, J. M. Alex, S. M. Amrutkar, A. T. Baviskar, G. Joshi, S. Singh, U. C. Banerjee, and R. Kumar, *Bioorg. Med. Chem.*, 2015, **23**, 5654.
24. M. V. P. dos Santos Nascimento, A. C. M. Munhoz, B. M. De Campos Facchin, E. Fratoni, T. A. Rossa, M. M. Sá, C. C. Campa, E. Ciraolo, E. Hirsch, and E. M. Dalmarco, *Biomed. Pharmacother.*, 2019, **111**, 1399.
25. T. G. Edwards and C. Fisher, *Antivir. Res.*, 2018, **152**, 68.
26. F. S. Macchi, K. Pissinate, A. D. Villela, B. L. Abbadi, V. Rodrigues-Junior, D. D. Nabinger, S. Altenhofen, N. Sperroto, A. da Siva Dadda, F. T. Subtil, T. F. de Freitas, A. P. Erhart Rauber, A. F. Borsoi, C. D. Bonan, C. V. Bizarro, L. A. Basso, D. S. Santos, and P. Machado, *Eur. J. Med. Chem.*, 2018, **155**, 153.

27. H. Mawasi, D. Bibi, and M. Bialer, *Bioorg. Med. Chem.*, 2016, **24**, 4246.
28. M. R. Wiley, L. C. Weir, S. L. Briggs, N. Y. Chirgadze, D. Clawson, D. S. Gifford-Moore, A. L. Schacht, G. F. Smith, V. Vasudevan, L. L. Zornes, and V. J. Klimkowski, *Bioorg. Med. Chem. Lett.*, 1999, **9**, 2767.
29. K. Sztanke, K. Pasternak, A. Sidor-Wójtowicz, J. Truchlińska, and K. Jóźwiak, *Bioorg. Med. Chem.*, 2006, **14**, 3635.
30. A. P. G. Nikalje, M. S. Ghodke, F. A. K. Khan, and J. N. Sangshetti, *Chin. Chem. Lett.*, 2015, **26**, 108.
31. S. Bretagne, *Antibiotiques*, 2009, **11**, 133.
32. Réseau algérien de surveillance de la résistance des bactéries aux antibiotiques. *Standardisation de l'antibiogramme à l'échelle nationale (médecine humaine et vétérinaire)*, 2011, 25.
33. E. Dannaoui, *Therapies*, 2006, **61**, 201.
34. F. Cheng, W. Li, Y. Zhou, J. Shen, Z. Wu, G. Liu, P. W. Lee, and Y. Tang, *J. Chem. Inf. Model.*, 2019, **59**, 4959.
35. T. Lynch and A. L. Price, *Am. Fam. Physician.*, 2007, **76**, 391.
36. R. Callaghan, F. Luk, and M. Bebawy, *Drug Metab. Dispos.*, 2014, **42**, 623.
37. J. D. Irvine, L. Takahashi, K. Lockhart, J. Cheong, J. W. Tolan, H. E. Selick, and J. R. Grove, *J. Pharm. Sci.*, 1999, **88**, 28.
38. D. A. Volpe, *Future Med. Chem.*, 2011, **3**, 2063.
39. A. Iraji, O. Firuzi, M. Khoshneviszadeh, H. Nadri, N. Edraki, and R. Miri, *Bioorg. Chem.*, 2018, **77**, 223.
40. A. S. Setlur, S. Y. Naik, and S. Skariyachan, *Interdiscipl. Sci. Comput. Life Sci.*, 2017, **9**, 254.
41. S. Bouaziz-Terrachet, A. Toumi-Maouche, B. Maouche, and S. Taïri-Kellou, *J. Mol. Model.*, 2010, **16**, 1919.
42. K. O. Lamara, M. Makhloufi-Chebli, A. Benazzouz-Touami, S. Terrachet-Bouaziz, N. Hamdi, A. M. S. Silva, and J. Bernard Behr, *J. Mol. Struct.*, 2021, **1231**, 129936.
43. S. Abbes, H. Trabelsi, I. Amouri, H. Sallemi, S. Nej, C. Fatma, F. Makni, and A. Ayadi, *Ann. Biol. Clin.*, 2012, **70**, 635.
44. N. Karaca and A. N. Koc, *Diagn. Microbiol. Infect. Dis.*, 2004, **48**, 259.
45. A. Lagunin, D. Filimonov, A. Zakharov, W. Xie, Y. Huang, F. Zhu, T. Shen, J. Yao, and V. Poroikov, *QSAR Comb. Sci.*, 2009, **28**, 806.
46. J. A. Castillo-Garit, Y. Marrero-Ponce, F. Torrens, and R. García-Domenech, *J. Pharm. Sci.*, 2008, **97**, 1946.
47. R. Liu, H. Sun, and S. S. So, *J. Chem. Inf. Comput. Sci.*, 2001, **41**, 1623.

48. G. Klopman, L. R. Stefan, and R. D. Saiakhov, *Eur. J. Pharm. Sci.*, 2002, **17**, 253.
49. F. Broccatelli, E. Carosati, A. Neri, M. Frosini, L. Goracci, T. I. Oprea, and G. Cruciani, *J. Med. Chem.*, 2011, **54**, 1740.
50. R. G. Susnow and S. L. Dixon, *J. Chem. Inf. Comput. Sci.*, 2003, **43**, 1308.
51. J. Wu, T. Ni, X. Chai, T. Wang, H. Wang, J. Chen, Y. Jin, D. Zhang, S. Yu, and Y. Jiang, *Eur. J. Med. Chem.*, 2018, **143**, 1840.
52. H. Kai-Cheng, C. Yen-Fu, L. Shen-Rong, and Y. Jinn-Moon, *BMC Bioinform.*, 2011, **12**, 1.
53. M. V. Keniya, M. Sabherwal, R. K. Wilson, M. A. Woods, A. A. Sagatova, J. D. Tyndall, and B. C. Monk, *Antimicrob. Agents Chemother.*, 2018, **62**.
54. Marvin Sketch program, Chemaxon, http://www.chemaxon.com, 2009.
55. S. Hammad, S. Bouaziz-Terrachet, R. Meghnem, and D. Meziane, *J. Mol. Model.*, 2020, **26**, 1.